Compensation of Nonlinearities in High-Density Magnetic Recording Channels

E. Biglieri, E. Chiaberto, G. P. Maccone, and E. Viterbo

Abstract—**Volterra-series models of magnetic-saturation recording channels are used to derive readback structures that compensate for channel nonlinearities. These structures are based on a canceler of linear and nonlinear channel distortions, and can achieve significant improvement in terms of mean-square error and error probability. Proper operation of the canceler requires reliable preliminary decisions to be taken on the information symbols. These decisions are obtained by passing the received signal through a linear equalizer, then processing the equalized signal through a symbol-by-symbol detector or a Viterbi detector. By using the data obtained in [4] for magneto-resistive heads, it was found that symbol-by-symbol preliminary detection performs adequately. A Volterra model was also obtained experimentally for the recording channel generated by magneto-inductive heads that exhibit higher-order nonlinear effects. In order to recover data from this highly distorted channel the preliminary detection scheme needs a 4-state Viterbi detector.**

I. Introduction

THE digital saturation magnetic recording channel has been widely studied by using a linear model (see, e.g., [1], [2]). Various detection methods based on the latter have been proposed to compensate for the presence of severe intersymbol interference (ISI) and of noise.

Various forms of write equalization have been proposed, with the aim of reducing ISI and facilitating the detection process at the cost of reducing the information recording density [5], [6], [7]. Readback equalization reduces ISI in a signal affected by noise (see, e.g., [1] and the references therein). The most common detection structures are inherently based on a linear model of the magnetic channel, and hence entail a loss of optimality as soon as nonlinear effects, due to high-density recording, become significant.

Volterra series are by now a tool widely used for modeling mildly nonlinear systems [12]. A third-order discrete Volterra series model for a digital magnetic recording saturation channel with magneto-resistive heads was recently proposed by Hermann [4], who also provided a method for Volterra kernel identification. The results in [4] show that the Volterra model matches the real channel well, especially with high recording density. Hirt [3] has applied to the nonlinear magnetic recording channel the optimal linear receiving filter proposed in [9].

A wide variety of detection methods are known for nonlinear transmission systems modeled by Volterra series. Among them, [10] generalizes the concept of decision feedback equalization, a technique long known to provide a good compromise between performance benefits and detector complexity [8]. This concept, called "nonlinear cancellation" in [10], is applied here to high-density, highly nonlinear magnetic recording channels. The idea is to form a model of the linear and nonlinear distortion introduced by the channel, and subtract it from the received signal. To do this, reliable preliminary decisions must be made available. They are obtained by passing the received signal through a linear equalizer, then processing the equalized signal through a preliminary detector. An interesting feature of these nonlinear cancellation methods is the possibility of simply adding the canceler device to the existing detection system for performance improvement.

Two different types of channels are considered here, based on magnetoresistive (MR) heads (Section II) or on magneto-inductive (MI) heads (Section III), respectively. In both cases, the readback system uses a nonlinear canceler. For the MR head examined here, a linear tapped-delay-line equalizer followed by a simple threshold (symbol-by-symbol) detection was adequate, while for the MI head a more refined preliminary detection scheme was required, using maximum-likelihood sequence estimation. Simulation results show a significant improvement over the simple linear equalizer, both in terms of mean square error and symbol error probability.

II. Compensating a Channel with MR Heads

We assume here that the magnetic recording channel $\mathcal{H}$ can be modeled as a discrete-time system with finite memory length $L = D + D'$, so that we are allowed to write

$$y_k = \mathcal{H}(x_{k-D}, \cdots, x_k, \cdots, x_{k+D'}), \tag{1}$$

where the symbols x_k take on values ± 1 and y_k are the samples observed at the output of the channel.

Based on the results in [4] we approximate the nonlin-

Manuscript received January 27, 1994; revised June 3, 1994.

G. P. Maccone is with Conner Peripherals Europe, Pont St. Martin, Italy.

E. Biglieri, E. Chiaberto, and E. Viterbo are with Dipartimento di Elettronica, Politecnico di Torino, I-10129 Torino, Italy.

IEEE Log Number 9403994.

TABLE I
VOLTERRA KERNELS FOR 56 kfci [4]

n	h_n	$c_n^{(1)}$	$c_n^{(2)}$	$c_n^{(3)}$	$c_n^{(1,2)}$
0	0.05	−0.005	0.005	0.001	−0.001
1	0.10	−0.010	0.007	−0.002	−0.002
2	0.20	−0.003	0.005	0.010	−0.005
3	0.60	−0.145	0.070	0.050	−0.125
4	1.00	−0.100	0.120	0.037	−0.080
5	−0.60	0.100	−0.020	0.001	0.120
6	−0.80	0.040	−0.010	0.000	0.070
7	−0.40	0.020	−0.005	0.004	0.030
8	−0.20	0.010	0.000	0.000	0.020
9	−0.10	0.005	0.000	0.000	0.000
10	−0.05	0.001	0.000	0.000	0.000

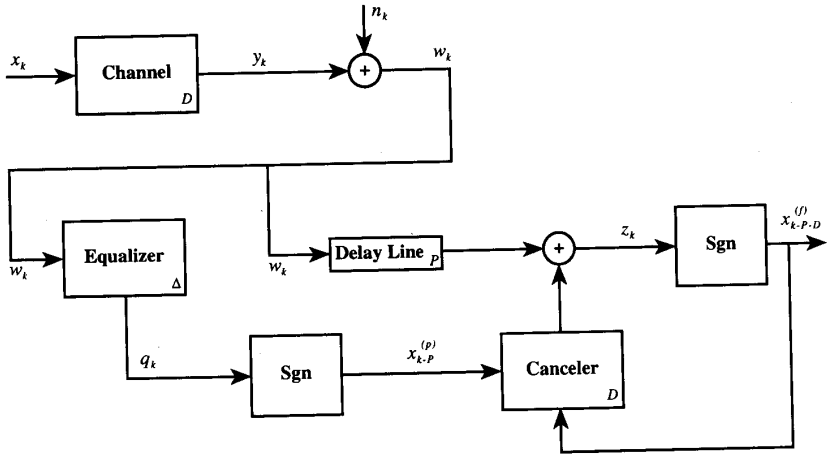

Fig. 1. The detection system. n_k represents white Gaussian noise. The letters D and Δ at the bottom right corner of the blocks denote the delay introduced by the block itself.

ear function $\mathcal{H}$ by the third-order Volterra series

$$y_{k+D} = \sum_{n=0}^{M} h_n x_{k+n} + \sum_{n=0}^{M} c_n^{(1)} x_{k+n} x_{k+n-1} + \sum_{n=0}^{M} c_n^{(2)} x_{k+n} x_{k+n-2} + \sum_{n=0}^{M} c_n^{(3)} x_{k+n} x_{k+n-3} + \sum_{n=0}^{M} c_n^{(1,2)} x_{k+n} x_{k+n-1} x_{k+n-2} \quad (2)$$

where $M = L - 3$ and h_n, $c_n^{(1)}$, $c_n^{(2)}$, $c_n^{(3)}$, $c_n^{(1,2)}$, for $n = 0, 1, \cdots M$, are the linear, second order, and third order Volterra kernels, respectively. These have been identified in [4] for different recording densities. We have taken these results for the highest density of 56 kfci (kilo flux changes per inch) as a model for the nonlinear channel (Table I), and we have applied our cancellation technique.

A. The Detection System

The detection scheme is shown in Fig. 1. The input symbols $x_k \in \{\pm 1\}$ represent the positive and negative saturation currents which magnetize the recording medium at a normalized rate $T^{-1} = 1$. Since we are interested in "raw" channel performance, we assume that no coding is used so that a binary information source is directly mapped onto the bipolar input according to the following rule: $0 \to -1$ and $1 \to +1$.

The channel introduces a fixed delay of D symbols. From the column labeled "h_n" in Table I we see that $D = 4$. The channel output is sampled at rate T^{-1} symbols per second, and white (i.e., independent and identically distributed) Gaussian noise samples n_k are added. The samples $w_k = y_k + n_k$ are processed by the detection system. The equalizer is a linear tapped-delay line with $N + 1$ taps. The values of its tap weights were calculated so as to minimize the mean square error [13, Section 10.6]

$$E\{|q_k - x_{k-D-\Delta}|^2\},$$

between its output sequence and the input symbols. Here q_k denotes the equalizer output, and Δ is the delay introduced by the equalizer, the optimal value of which was found to be $N/2$ in all cases tested. Since the symbols w_k follow two different paths, these must introduce the same

delay $P = \Delta + D$ caused by the equalizer and the canceler, so that a P-symbol delay must be introduced.

The 'Sgn' block performs a zero-threshold decision on its input and produces bipolar outputs, which are the preliminary and final decisions on the corresponding input symbols, denoted $x^{(p)}_{k-P}$ and $x^{(f)}_{k-P-D}$, respectively.

With the aid of Fig. 2 we may take a closer look at the structure of the canceler. It aims at subtracting the linear and nonlinear ISI terms from the output of the delay line before final decisions on the transmitted symbols are made.

Equation (1) can be rewritten in the following form:

$$y_k = h_D x_k + \mathcal{F}(x_{k-D}, \cdots, x_k, \cdots, x_{k+D'}) \quad (3)$$

where

$$\mathcal{F}(x_0, \cdots, x_L) = \sum_{n=0, n\neq D}^{M} h_n x_n + \sum_{n=0}^{M} c_n^{(1)} x_n x_{n+1} + \sum_{n=0}^{M} c_n^{(2)} x_n x_{n+2} + \sum_{n=0}^{M} c_n^{(3)} x_n x_{n+3} + \sum_{n=0}^{M} c_n^{(1,2)} x_n x_{n+1} x_{n+2} \quad (4)$$

where, as before, L denotes the channel memory.

In principle, if the model (4) were exact and the canceler fed with correct decisions on the input symbols, then all the ISI terms would be subtracted, and the system would be degraded by additive Gaussian noise only. However, if some of the decisions in the canceler are incorrect, then ISI is removed only in part, and some spurious terms with the wrong spin appear. As we shall see in the next section, the effectiveness of this technique largely depends on the reliability of the preliminary decisions used to feed the canceler. For this reason the canceler is fed, where possible, by the final decisions, which are more reliable than the preliminary ones. This is the concept of "decision feedback." The canceler (Fig. 2) actually works as follows: 1) the final decision $x^{(f)}_{k-P-D}$ is fed back at location D of the shift register, and overwrites the old preliminary decision, 2) the new preliminary decision $x^{(p)}_{k-P+1}$ is shifted into location 0, 3) the function $\mathcal{F}$ is applied to the content of the register, and 4) the result is subtracted from the delayed readback symbol w_k.

B. Simulation Results

In this section we discuss the results of the computer simulations run based on the above model. The goal here is to evaluate the performance of the system in terms of mean-square error (MSE) and error probability $P(e)$ for different values of SNR. The latter is defined as the ratio between $E\{y_k^2\}$ and the noise power σ^2, taken in dB.[1]

In general, the mean square errors $E\{|q_k - x_{x-P}|^2\}$ and $E\{|x_k - x_{k-P-D}|^2\}$ are calculated more easily than error probabilities: however, they do not provide a true performance measure since the sporadic symbol errors influence very modestly their final value. Nevertheless, MSE provides a rough measure of the possible gains in terms of $P(e)$.

[1]The signal energy $E\{y_k^2\}$ is about 2.7 here, since the Volterra kernels were not normalized to obtain unit output energy.

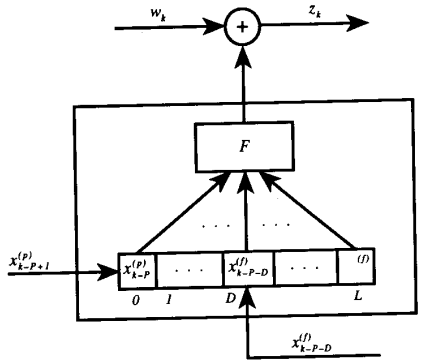

Fig. 2. The canceler.

Figs. 3 and 4 show the limitations of linear equalization as the number of taps increases. It turns out that increasing the length of the equalizer will produce diminishing gains above a certain limit—this is partly due to the nonlinear behavior of the channel. To go beyond this limit, we advocate introduction of nonlinear cancellation.

Figs. 5 and 6 show how a nonlinear canceler outperforms a 9-tap linear equalizer. The same linear equalizer was used to generate preliminary decisions. It is interesting to note that the two curves cross over at a certain point. This is due to the negative effects of error propagation for low SNRs. To evaluate more carefully where this cross-over takes place, it is instructive to examine error probability curves. They show that cross-over takes place only at relatively large values of $P(e)$, and consequently in normal conditions the introduction of a canceler actually improves performance.

III. Compensating a Channel with MI Heads

The MI head examined here generates a channel with greater tails and higher-order nonlinear terms than MR heads. The simple symbol-by-symbol detection scheme, which was effective with the head considered in the previous section, is inefficient here, and simulation results showed that the weakness of such a scheme lies in the low quality of the preliminary decisions. This is due to the excessive strain imposed on the equalizer.

To solve the compensation problem for this channel we consider an equalizer which approximately transforms the overall impulse response (channel + equalizer) into a simple partial-response channel. This reduces significantly the residual error after the equalizer, but requires that maximum-likelihood sequence estimation (MLSE) be used for preliminary decisions (note that these are not optimum, since the noise is not white at the equalizer output). In practice the latter is implemented by using the truncated Viterbi algorithm, whose complexity (number

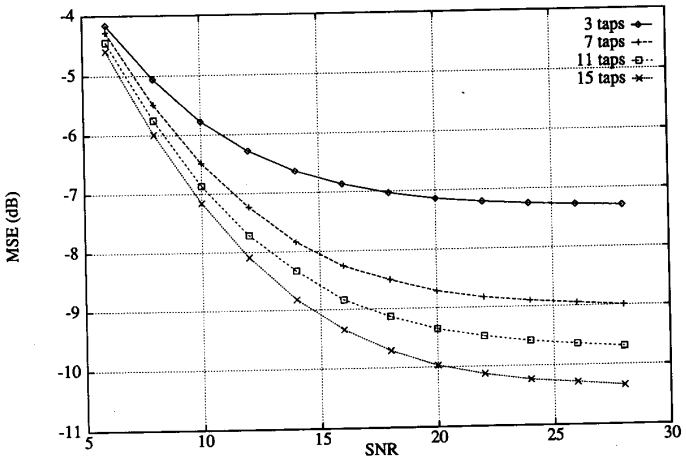

Fig. 3. MSE at the output of a linear equalizer with 3, 7, 11, and 15 taps.

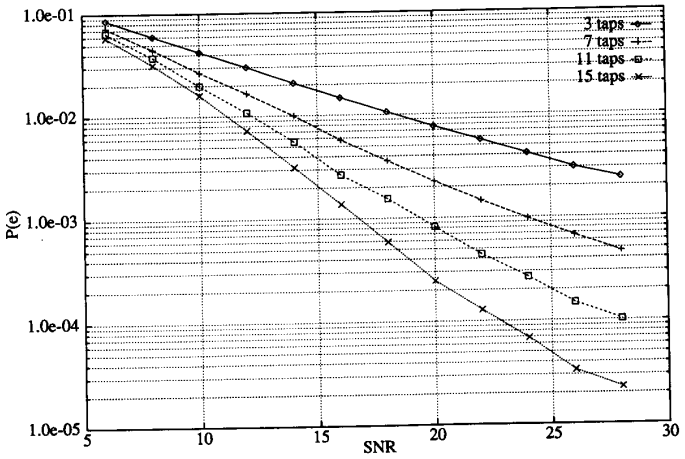

Fig. 4. $P(e)$ at the output of a linear equalizer with 3, 7, 11, and 15 taps.

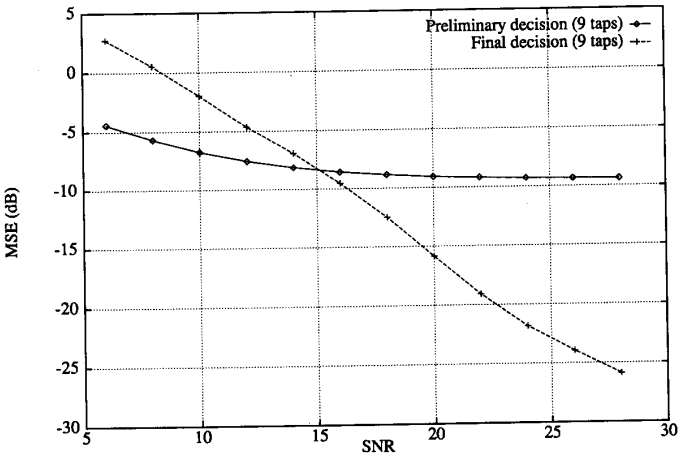

Fig. 5. MSE before preliminary and final decisions with a 9-tap linear equalizer.

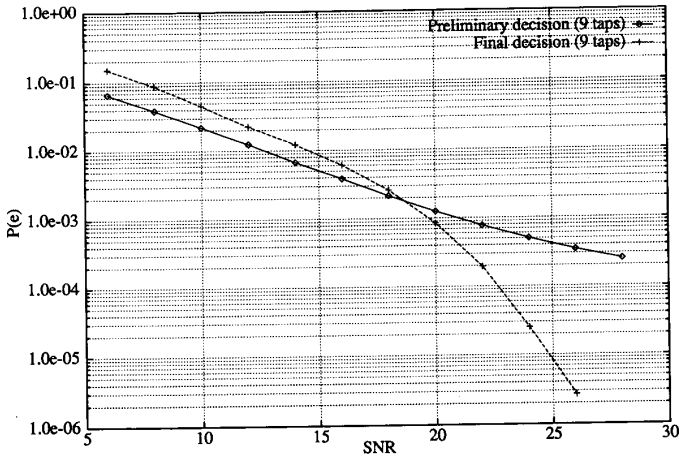

Fig. 6. $P(e)$ after preliminary and final decisions with a 9-tap linear equalizer.

of states) grows exponentially with the memory length of the partial-response channel.

In the following we show that preliminary detection based on a four-state Viterbi receiver, combined with a nonlinear canceler, is sufficient to achieve the desired quality. Another four-state Viterbi receiver is used to obtain final decisions. With this structure, final decisions are not fed back into the canceler. This is because the Viterbi algorithm introduces a delay, and hence final decisions are not available at the right time to be fed back.

An alternative to this structure would be based on the "delayed decision-feedback sequence estimation" concept proposed in [11]. By using this we could eliminate one of the Viterbi detectors and use the decisions given by the ML path to feed the canceler, which in turn can touch up the branch metrics in the Viterbi detector. The total decoding delay would also be reduced. The problem is that in order to account for all the precursors of the impulse response we would need at least a 16-state sequence estimator, as opposed to two 4-states sequence estimators, and consequently a higher complexity.

A. The Magnetic Recording Channel with MI Heads

A Volterra model for the magnetic channel with MI heads was identified by using standard techniques [4]. The nonlinear function $\mathfrak{IC}$ in (1) was approximated by the following third-order Volterra series

$$y_{k+D} = \sum_{n=0}^{M} h_n x_{k+n} + \sum_{n=0}^{M} c_n^{(1,2)} x_{k+n} x_{k+n-1} x_{k+n-2} \quad (5)$$

$$+ \sum_{n=0}^{M} c_n^{(2,3)} x_{k+n} x_{k+n-2} x_{k+n-3}$$

$$+ \sum_{n=0}^{M} c_n^{(1,3)} x_{k+n} x_{k+n-1} x_{k+n-3} \quad (6)$$

where $M = L - 3$ and h_n, $c_n^{(1,2)}$, $c_n^{(2,3)}$, $c_n^{(1,3)}$, for $n = 0, 1 \cdots M$, are the linear, and third order Volterra kernels, respectively. The measured values are reported in Table II. We note the absence of any relevant second order Volterra kernels: this is due to the symmetry between the positive and negative pulses of the impulse response, a typical feature of MI heads.

TABLE II
VOLTERRA KERNELS FOR 88 kbpi MI HEADS

n	h_n	$c_n^{(1,2)}$	$c_n^{(2,3)}$	$c_n^{(1,3)}$
0	0.1357	0.0148	0.0166	−0.0115
1	0.5608	−0.0178	0.0035	−0.0095
2	0.9982	−0.0693	−0.0033	−0.0212
3	−0.0289	−0.1611	−0.0139	−0.0074
4	−0.8750	−0.0729	−0.0543	0.0424
5	−0.4865	0.1415	−0.0342	0.0383
6	−0.2115	0.1046	0.0454	−0.0170
7	−0.0433	0.0409	0.0404	−0.0189

B. The Detection System

The detection scheme we propose for the recording channel with MI heads is shown in Fig. 7. The input symbols $x_k \in \{\pm 1\}$ denote the positive and negative saturation currents which magnetize the recording medium at a normalized rate $T^{-1} = 1$. As before we assume no coding, so that the binary information source is directly mapped onto the bipolar input according to the rule $0 \rightarrow -1$ and $1 \rightarrow +1$.

From Table II, column labeled "h_n," we see that the delay D introduced by the channel is equal to two input symbols. The signal w_k, through two different routes, is used for preliminary decisions and for ISI cancellation. Fig. 8 shows the desired impulse response to be obtained after equalization. Here d_k is the desired output of the equalized channel. For our MI head the choice $d_k = x_k$, which worked well for the MR head of previous chapter, gives poor results because the equalizer does not provide

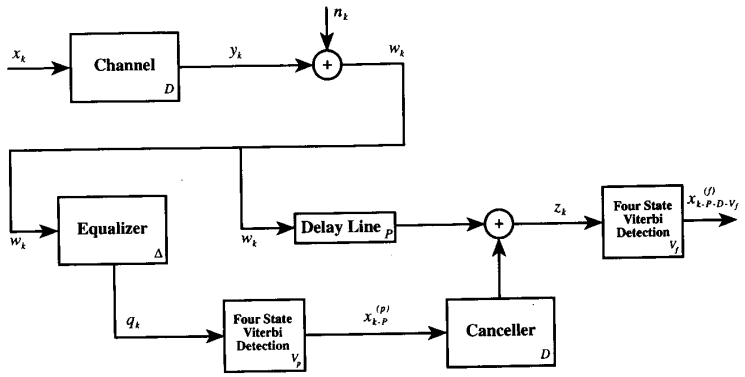

Fig. 7. The detection system for MI heads.

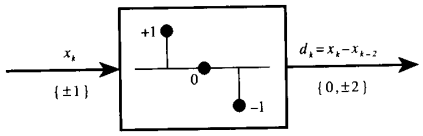

Fig. 8. The desired impulse response of channel + equalizer.

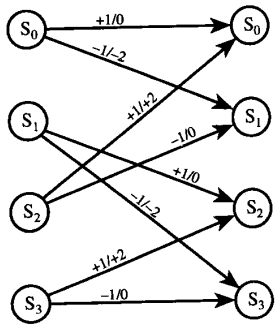

Fig. 9. Trellis of the MSLE.

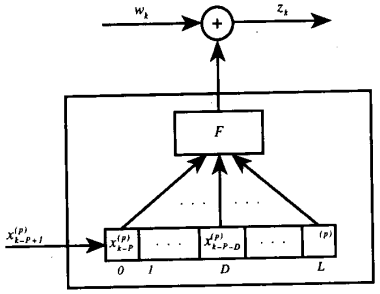

Fig. 10. The canceler.

an output signal clean enough to take reliable preliminary decisions. The equalizer's task is made easier with the choice of Fig. 8, at the price of not allowing symbol-by-symbol preliminary decisions.

The equalizer is a linear tapped delay line with $N + 1$ taps. The value of its tap weights were calculated so as to minimize the mean square error

$$E\{|q_k - x_{k-D-\Delta} + x_{k-D-\Delta-2}|^2\}$$

between the input and the output sequence, just as we did in the previous section. Here q_k denotes the equalizer output, and Δ is the delay introduced by the equalizer, which was found to take on the optimal value $N/2$. Optimal detection for the channel in Fig. 8 in the presence of additive white Gaussian noise requires a four-state Viterbi receiver, whose trellis is shown in Fig. 9. The labels on its branches denote the transmitted symbol and the corresponding channel output value, respectively. In practice, a truncated Viterbi algorithm is used with a decoding window $V_p = 12$; as for $V_p > 12$ no further improvement in the detection quality was experienced. The output $x_{k-P}^{(p)}$ of this Viterbi detector provides preliminary decisions on the corresponding input symbol x_{k-P}.

Since the symbols w_k follow two different routes, these must introduce the same delay $P = D + \Delta + V_p$ caused by the equalizer, the preliminary detection and the canceler, so that a P-symbol delay line is required. Fig. 10 shows the canceler, which cancels linear and nonlinear channel response except its desired part.

Equation (1) can be rewritten in the following form:

$$y_k = x_k - x_{k-2} + \mathcal{F}(x_{k-D}, \cdots, x_k, \cdots, x_{k+D'}) \quad (7)$$

where

$$\begin{aligned}\mathcal{F}(x_0, \cdots, x_L) &= (-1 + h_D)x_D + (1 + h_{D+2})x_{D+2} \\ &+ \sum_{\substack{n=0 \\ n \neq D, D+2}}^{M} h_n x_n + \sum_{n=0}^{M} c_n^{(1,2)} x_n x_{n+1} x_{n+2} \\ &+ \sum_{n=0}^{M} c_n^{(2,3)} x_n x_{n+2} x_{n+3} + \sum_{n=0}^{M} c_n^{(1,3)} x_n x_{n+1} x_{n+3},\end{aligned} \quad (8)$$

where, as before, L denotes the channel memory.

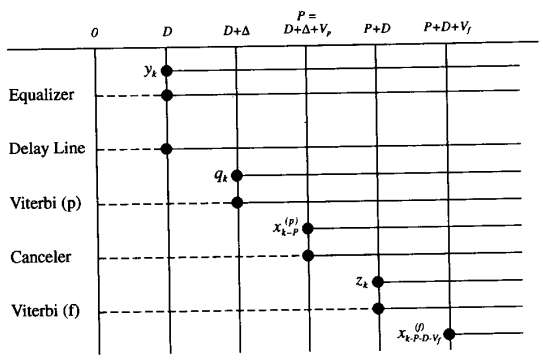

Fig. 11. Timing of the readback system.

Finally the four-state Viterbi detection block, with decoding delay V_f, outputs the final decisions $x^{(f)}_{k-P-D-V_f}$ on the corresponding input symbols $x_{k-P-D-V_f}$.

Fig. 11 summarizes the delays introduced by each block. The total readback delay for the final decision is $D + \Delta + V_p + D + V_f$. With a five tap equalizer and optimum detection windows in the Viterbi blocks ($V_p = V_f = 12$), we have a total delay of 30 input symbols.

Some further comments on the type of errors that appear in the system are in order here. A detection failure of MLSE results, in general, in an error burst at its output. Error bursts in preliminary decisions do propagate in the canceler, thus producing a highly degraded signal at the input of the final Viterbi detector. Our simulation results have shown that on the average the final Viterbi detector is able to recover quite well from this type of situation, which results in a lower error probability for final decisions. In the attempt of breaking the error bursts at the output of the preliminary Viterbi detector, an interleaver/deinterleaver scheme was also considered. By placing an interleaver before the channel we transform the system into a periodically time-varying system with period depending on the interleaving depth. This requires a number of cancelers equal to the interleaving depth, which should be fed by a deinterleaver placed at the output of the preliminary Viterbi detector. Since the error bursts we want to break could be typically around eight symbols long, the sheer number of cancelers introduces an unacceptable complexity.

C. Simulation Results

We now evaluate the performance of the system in terms of mean-square error $E\{|q_k - x_{k-P} + x_{k-P-2}|^2\}$ and $E\{|z_k - x_{k-P-D-V_f} + x_{k-P-D-V_f-2}|^2\}$, and of error probability $P(e)$.[2]

Figs. 12 and 13 show the limitations of linear equalization as the number of taps increases. It turns out that increasing the length of the equalizer produces diminishing gains, in terms of MSE, above a certain limit—this is due in part to the nonlinear behavior of the channel. When we look at the error probability we see that increasing the length of the equalizer above 5 produces unpredictable negative effects on the preliminary decision. Figs. 14 and 15 show the performance improvement obtained by a nonlinear canceler with respect to 5-tap linear equalizations. In particular we have a gain of about 0.7 dB at 10^{-5} error

[2]The signal energy $E\{y_k^2\}$ is about 2.5 here.

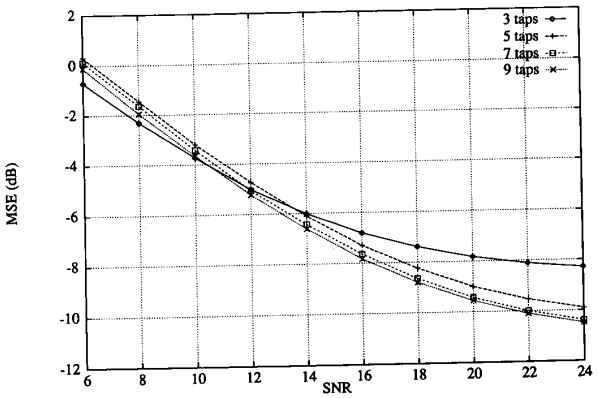

Fig. 12. MSE at the output of a linear equalizer with 3, 5, 7 and 9 taps.

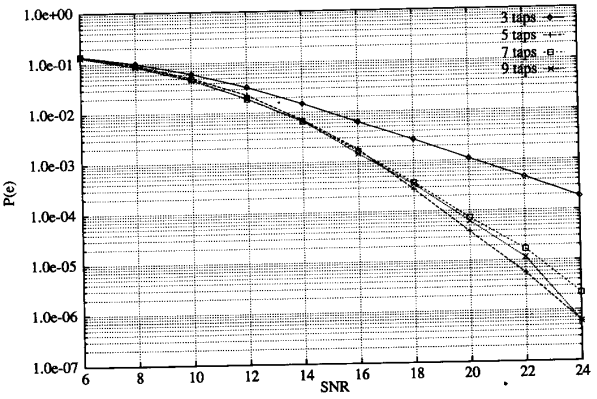

Fig. 13. $P(e)$ at the output of a linear equalizer with 3, 5, 7 and 9 taps.

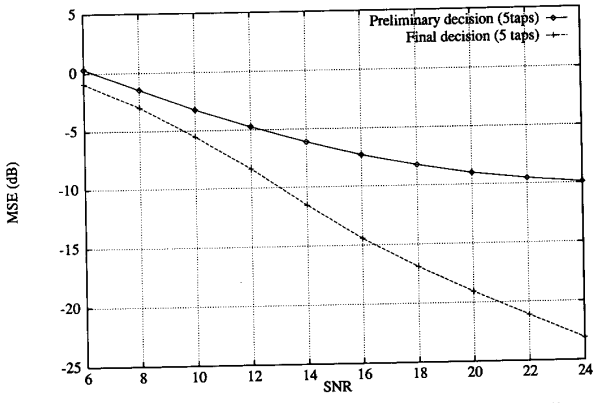

Fig. 14. MSE before preliminary and final decisions with a 5-tap linear equalizer.

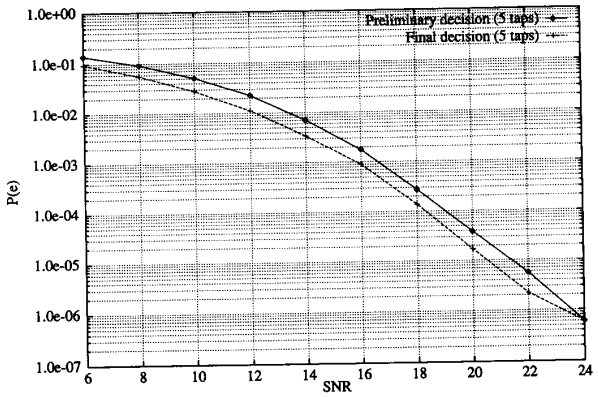

Fig. 15. $P(e)$ after preliminary and final decisions with a 5-tap linear equalizer.

probability. We expect this gain to be higher as the channel becomes more nonlinear: however, our experimental setup did not allow the identification of channels with a higher recording density.

IV. Conclusions

New readback systems, organized in the form of an add-on feature, were presented for high-density magnetic recording systems. Nonlinear channels were modeled by using third-order Volterra series. Channels whose behavior is more nonlinear require a more complex detection scheme to obtain the reliable preliminary decisions that are necessary for proper operation of the canceler.

References

[1] W. M. Bergmans, "Density improvements in digital magnetic recording by decision feedback equalization," *IEEE Trans. Magn.*, vol. 22, no. 3, pp. 157–162, May 1986.

[2] J. Moon and L. R. Carley, "Performance comparison of detection methods in magnetic recording," *IEEE Trans. Magn.*, vol. 26, no. 6, pp. 3155–3172, Nov. 1990.

[3] W. Hirt, "The optimal linear readback filter for nonlinear magnetic recording channel," to be published.

[4] R. Hermann, "Volterra modeling of digital magnetic saturation recording channels," *IEEE Trans. Magn.*, vol. 26, no. 5, pp. 2125–2127, Sept. 1990.

[5] R. C. Schneider, "Write equalization in high-density magnetic recording," *IBM J. Res. Dev.*, vol. 29, no. 6, pp. 563–568, Nov. 1985.

[6] ——, "Write equalization for generalized (d, k) codes," *IEEE Trans. Magn.*, vol. 24, no. 6, pp. 2533–2535, Nov. 1988.

[7] H. D. L. Hollmann, "The general solution of write equalization for RLL (d, k) codes," *IEEE Transactions Information Theory*, vol. 37, no. 3, pp. 856–862, May 1991.

[8] C. A. Belfiore and J. H. Park, Jr., "Decision feedback equalization," *Proceed. IEEE*, vol. 67, no. 8, pp. 1143–1156, Aug. 1979.

[9] E. Biglieri, M. Elia, and L. Lo Presti, "The optimal linear receiving filter for digital transmission over nonlinear channels," *IEEE Trans. Information Theory*, vol. 35, no. 3, pp. 620–625, May 1989.

[10] E. Biglieri, A. Gersho, R. D. Gitlin, and T. L. Lim, "Adaptive cancellation of nonlinear intersymbol interference for voiceband data transmission," *IEEE J. Selected Areas Comm.*, vol. SAC-2, no. 5, pp. 765–777, Sept. 1984.

[11] A. Duel-Hallen and C. Heegard, "Delayed decision-feedback sequence estimation," *IEEE Trans. Comm.*, vol. 37, no. 5, pp. 428–436, May 1989.

[12] M. Schetzen, *The Volterra and Wiener Theories of Nonlinear Systems*. New York: Wiley, 1980.

[13] S. Benedetto, E. Biglieri, and V. Castellani, *Digital Transmission Theory*. Englewood Cliffs: Prentice-Hall, 1987.

Ezio Biglieri (M'73–SM'82–F'89) was born in Aosta, Italy, in 1944. He received the Dr. Eng. degree in Electrical Engineering (*summa cum laude*) from Politecnico di Torino, Italy, in 1967.

He was a Professor of Electrical Engineering first with Università di Napoli, then with Politecnico di Torino, with University of California at Los Angeles, and again with Politecnico di Torino. He is a co-author of four books on digital communications, including the recent "Introduction to Trellis-Coded Modulation with Applications," published by Macmillan in 1991. His current research interests span digital communication theory, coded modulations, and applications of digital signal processing to telecommunications.

Elena Chiaberto was born in Aosta, Italy, in 1969.

A student of Electrical Engineering at Politecnico di Torino, she is presently working on her graduation report in collaboration with Conner Peripherals Europe on applications of Volterra series to nonlinear magnetic-recording channels.

Gian Pietro Maccone was born in Roma, Italy, in 1942. He graduated in physics and electrical engineering at the University of Roma.

From 1971 to 1987 he was with Olivetti, where he worked on magnetic hard-disk drives. Since 1988 he has been with Conner Peripherals Europe, Pont Saint Martin (Italy), involved with new hard-disk development.

Emanuele Viterbo was born in Torino, Italy, in 1966. He received his degree in Electrical Engineering in 1989 from Politecnico di Torino, Italy.

For two years he was with the European Patent Office, The Hague, Holland, as a patent examiner in the field of dynamic recording and in particular of error-control coding. In 1992 he started his doctoral studies in Electrical Engineering at Politecnico di Torino. His current interests are in lattice codes, algebraic coding theory, digital terrestrial television broadcasting, and digital magnetic recording.